

Experimental data about mechanical behaviour during compression tests for various matted fibres

D. POQUILLON*, B. VIGUIER, E. ANDRIEU
CIRIMAT UMR 5085, ENSIACET-INPT, 31077 Toulouse Cedex 4, France
E-mail: Dominique.Poquillon@ensiacet.fr

A specific experimental device has been set up to test compressive mechanical behaviour of an assembly of fibres. Simple compression, as well as cyclic loading experiments and relaxation tests were performed. The experimental set up also allows to record the evolution of the mat fibre electrical resistance while testing. Experimental results are presented for a variety of fibrous materials. Despite the very different nature of each of these individual fibres, it appears that the mats exhibit a very similar mechanical behaviour. This common behaviour has been observed during monotonic single compression tests, as well as during cyclic or relaxation experiments. These experimental results are discussed in terms of different parameters such as the intrinsic mechanical properties of individual fibres and moreover the tangle intrinsic parameters (effect of fibre length, effect of geometrical position of fibres in the sample, fibre surface modifications. . .). The influence of the contact points between fibres is discussed in regard of the electric resistivity measurements. © 2005 Springer Science + Business Media, Inc.

1. Introduction

Studies devoted to cellular materials are numerous because of their specific properties [1, 2]. Besides, entangled materials are widely used (mutton wool mattress, glass wool for insulating. . .) but very few studies are devoted to the mechanical behaviour of such materials. However some data are available about the wood fibres [3, 4] or glass fibres [5]. On the other hand, theoretical simulations have been carried out on set of fibres in order to understand the effect of microstructural parameters on the mechanical behaviour in compression of these materials [6–9]. These materials can be characterised as a mechanical set of long elements entangled together, long means that their diameter is at least 2 decades smaller than their length. In all the tests carried out, no wetting effect were evidenced which may change fibres contacts or create internal pressure. So we would like to emphasise that these experiments lead to original mechanical behaviour, which differs, from the mechanical behaviour in compression of polymer or composite materials during production processes. In those cases, liquid between chain or fibres strongly influence the rheology of the assembly.

In this study, we investigated experimentally the mechanical behaviour of various matted fibres. Two cases have been studied: entangled isolated fibres (steel wools, human hair, sheep wool, carbon nano tube. . .) and wick of fibres (cotton). In all the tests carried out in the present study, the fibres motion and rearrangement is

a key point as the relative density of the matted fibres is always small, ranging from 5 to 20% of the fibre density.

2. Experimental device and methodology

Compression tests have been carried out on fibres and wicks of fibres which diameter ranges from 50 nm (carbon nano tube, see Fig. 1a) to 2 mm for vegetable horsehair. Table 1 gives the list of the fibres tested, their typical diameter for cylindrical fibres, their width and thickness for fibres having a rectangular section.

Glass wool tested was taken from commercial insulating material and has a regular cylindrical shape. On the contrary, vegetable horsehair used as padding in armchairs showed a large scatter in the diameter of the fibres. Cotton fibres (Fig. 1b) are raw materials, they have an 8-shape section and are covered with a natural coating of fat constituent. By contrast, wick of cotton are made from washed cotton twisted together (Fig. 2a). For the steel wools tested, shavings are manufactured by machining with different size but a rectangular section (Fig. 2b). The sheep wool has a round section and is also covered by suet (Fig. 3a). As compared to sheep wool, human hairs (Fig. 3b) tested are stiffer and their diameter larger, no occurrence of suet nor fat was noticed on human hair.

The samples were observed with a scanning electron microscope (LEO435VP) operating at 15 kV and

*Author to whom all correspondence should be addressed.

MECHANICAL BEHAVIOR OF CELLULAR SOLIDS

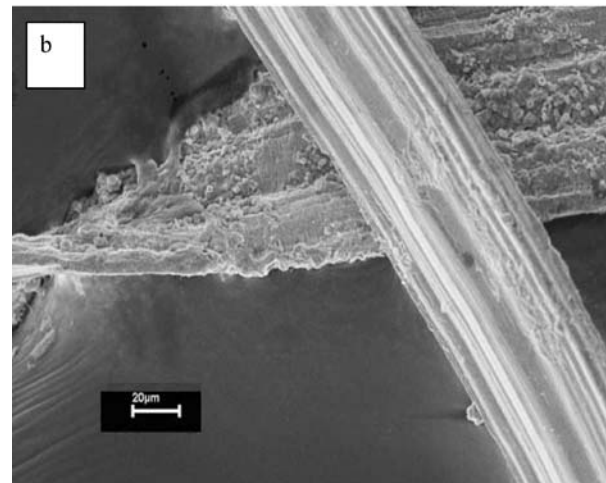
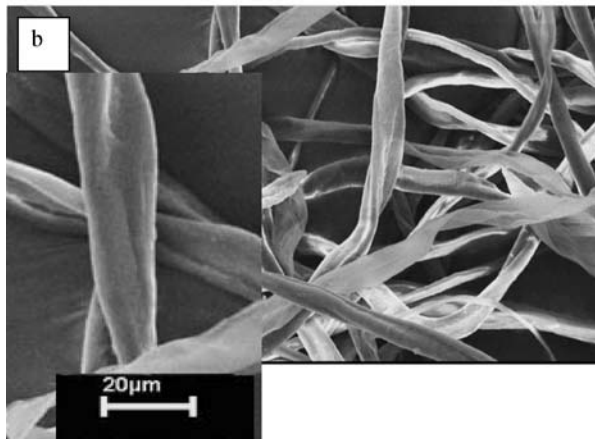
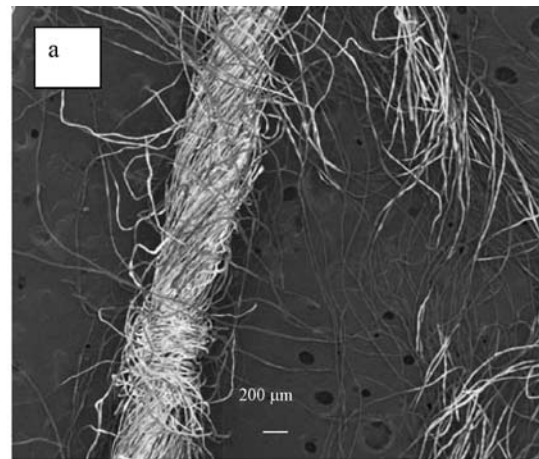
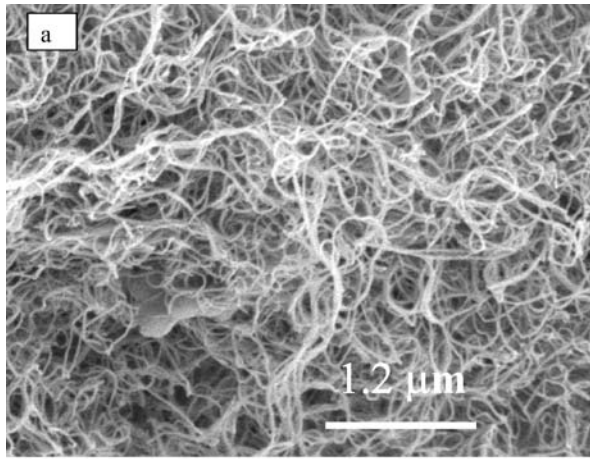


Figure 1 Microstructure of the fibres used in the study, as observed by SEM: (a) carbon nanotubes, (b) raw cotton fibres.

Figure 2 SEM observation of the fibres microstructure: (a) a wick of cotton, (b) steel wool n°000000.

reduced beam current. The fibers were just deposited on conductor tape.

A specific experimental apparatus has been set up to test compressive mechanical behaviour of an assembly of fibres (Fig. 4a). The mat is contained within a Plexiglass cylinder of 60 mm diameter. Compression is achieved with a MTS tension compression machine. The displacement is imposed and the load is measured (maximum 2kN). In the same time, a 4-point electrical resistance measurement is performed using an HP/Agilent 34970A Data Control Unit. Electric current is imposed, tension is measured and the electric resistance of the sample is calculated. Resistance could only be measured in a 10^{-3} – 10^8 ohm range which was not large enough for all the samples.

For glass wool, human hair, dry cotton, the electrical resistance of the sample was too high to be measured. On the contrary, for carbon nano tubes, we approach the lower limit of the device. For cotton fibres or human hair, few mg of water were sprayed on the sample in order to get enough conductivity to achieve measure-

ments. This water treatment influences the mechanical behaviour of the sample but this point will be discussed later.

Before each individual test, the material is carded manually, the carbon nano tubes which appear as a thin black powder were stirred using a glass stick. The position of the lower part of the metallic support is used as the zero position of the sample length. The carded sample is introduced between the lower and the upper part of the device (see Fig. 4b) and a compressive preloading of 2N is applied. This mechanical state defines the reference length of the sample l_0 . Then the displacement is imposed at a given rate. Different displacement rates have been tested : 0.6, 6 and 60 mm/min. The 6 mm/min displacement rate corresponds to a strain rate of about 10^{-3} s $^{-1}$. At a fixed load (e.g. 100 N) a dwell or an unloading is imposed. The unloading is stopped at the same value (2N) that the value used for the preload and the permanent strain obtained can be analysed.

TABLE I Fibres used in mattresses tested in the present study

Fibres	Carbon nano tube	Glass wool	Steel wool n°00000	Steel wool n°2	Mutton wool	Human hair	Vegetable horsehair	Cotton fibre	Wick of cotton fibre
Diameter or thickness (μm)	0.05	1–2	5	15	20	70	20–2000	20	1000
Width (μm)			20	50					

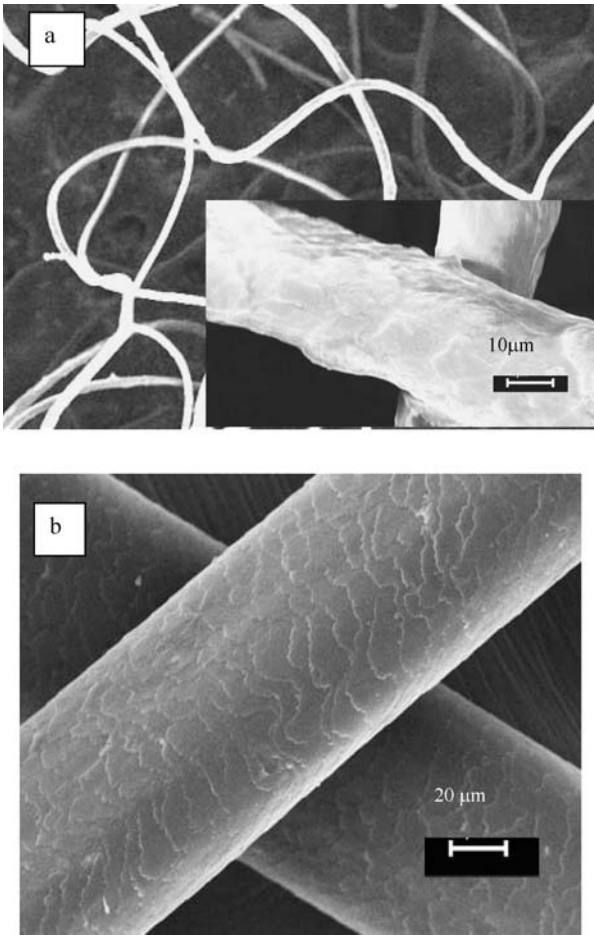


Figure 3 (a) SEM micrographs of mutton wool. (b) SEM micrograph of human hair.

To analyse the experimental results, we used the usual following definition for the stress σ and the true strain ε :

$$\varepsilon = \ln(l/l_0) \quad (1)$$

$$\sigma = F/S_0 \quad (2)$$

Note that, due to the experimental device, the specimen sections remains constant during the test. The electrical resistance R of the sample can be linked to the electrical resistivity ρ_e by:

$$\rho_e = RS_0/l \quad (3)$$

3. Experimental results

Fig. 5 gathers compression curves obtained on the various materials tested in this study. These data about the mechanical behaviour of various entangled fibres have been obtained during compression tests carried out at a 6 mm/min displacement rate. Unload is performed at the same rate as soon as the maximum load (here 100 N that corresponds to a 35370 Pa stress) is reached.

The shape of the curve is comparable for all the materials tested. A remanent strain is noticed for all the materials, due to the rearrangement of the fibres during this first compression cycle. Glass wool has the

larger residual strain, which is likely to be due to the regular shape of the fibres and to their smooth surface, which minimize friction stresses. Human hairs are also elastic fibres with both regular shape and surface so that entangled human hair achieved large compression. Curves obtained for raw cotton fibres and sheep wool are similar and we choose to plot only the mutton wool data on Fig. 5. The humid raw cotton achieved slightly higher compression than the dry one (in average 115% instead of 105%). Water content is known to increase elasticity of the cellulose as well as that of the keratin (human hair). Thus a higher humidity rate is supposed to enhance the bending properties of these organic fibres and consequently improving their capacity to be compressed. However, this is a minor effect as compared to the scattering of the results, which is inherent to the initial morphology of the set of entangled fibres (microstructural effect). This humidity of the fibres was needed to achieve electrical measurements as detailed in another paragraph.

For the wick of cotton, we investigated the effect of the length of the wick on the mechanical response of the sample in compression. When the wicks length is below the diameter of the cylinder, no size effects can be reported whereas they become noticeable when wicks are long compared to the diameter of the device. Compression rate achieved at the same load are then smaller with longer wicks. This point means that the results we get with steel wool and cotton wick can be dependent on the size of the apparatus contrary to the results obtained for the other fibres tested.

3.1. Effect of the load level

We wonder if the residual strain was dependent on the maximum load reached. In fact, as illustrated on Fig. 6 for mutton wool, increasing the load level gives the same master curves and furthermore the residual strain appears to be quite constant for the elastic fibres tested in that conditions (mutton wool, raw cotton, wick of cotton, vegetable horsehair) whereas it is clearly dependent on the load level reached for the two steel wools tested.

This point clearly indicates that the macroscopic compression curves obtained is due to the morphology of the assembly and to the relative motion and friction of the fibres. The non-linearity of the curve cannot be explained solely by the individual behaviour of the fibre. Since the data available (glass wool, carbon nano tube) and the traction tests performed in our laboratory on isolated fibres (human hair, mutton wool, raw cotton) confirm that these fibres follow a linear elastic behaviour in the beginning of the traction tests. On the other hand, steel wool fibres have plastic zones with permanent strain before any test (Fig. 2b). These knees can promote strain localisation provided that the strain hardening of the corresponding steel is weak.

3.2. Electrical resistance

Compression tests have been carried out several time on the same sample (carded between each test) on mutton

MECHANICAL BEHAVIOR OF CELLULAR SOLIDS

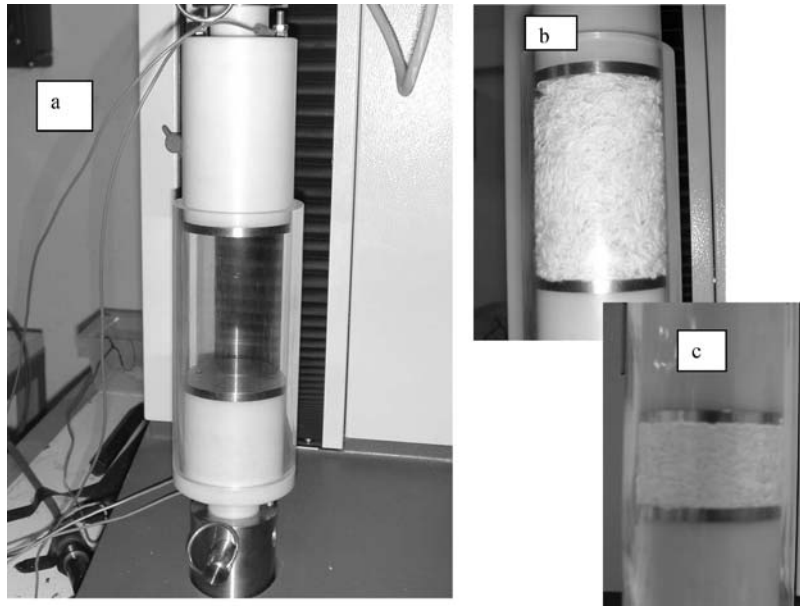


Figure 4 A general view of the experimental device showing the plexiglass tube in which the fibres are enclosed (a) and details of a mattress made of wick of cotton in the tube at the end of the preloading step ($F = -2\text{ N}$) (b) and under compression ($F = -100\text{ N}$) (c).

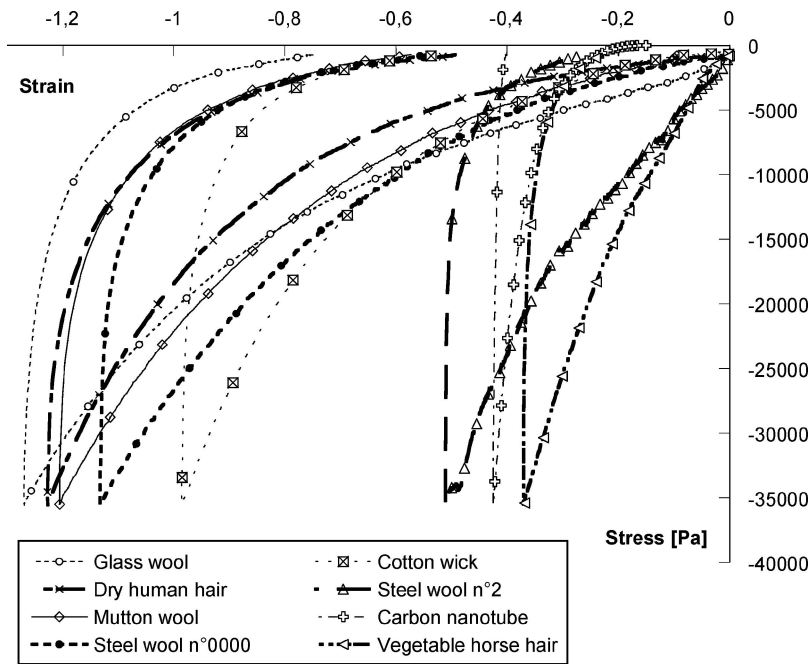


Figure 5 Stress–strain curves for compression tests carried out at 6 mm/min until 100 N before unloading at the same rate.

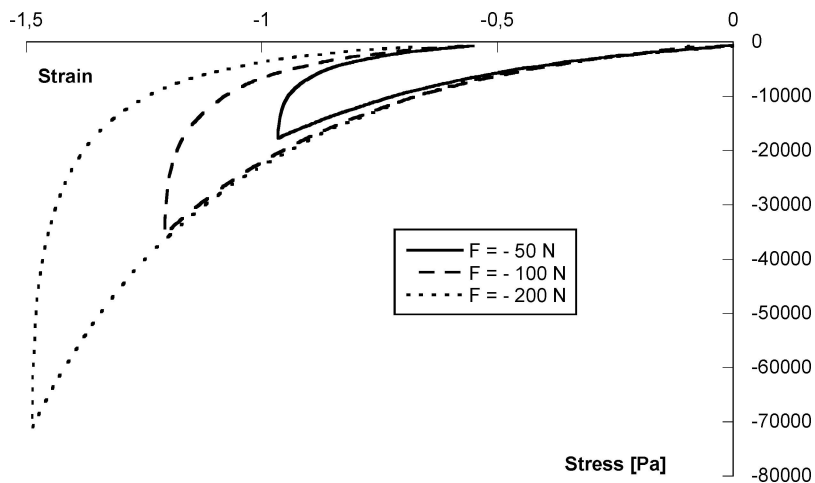


Figure 6 Stress–strain curve for compression tests carried out at different load level at 6 mm/min on mutton wool.

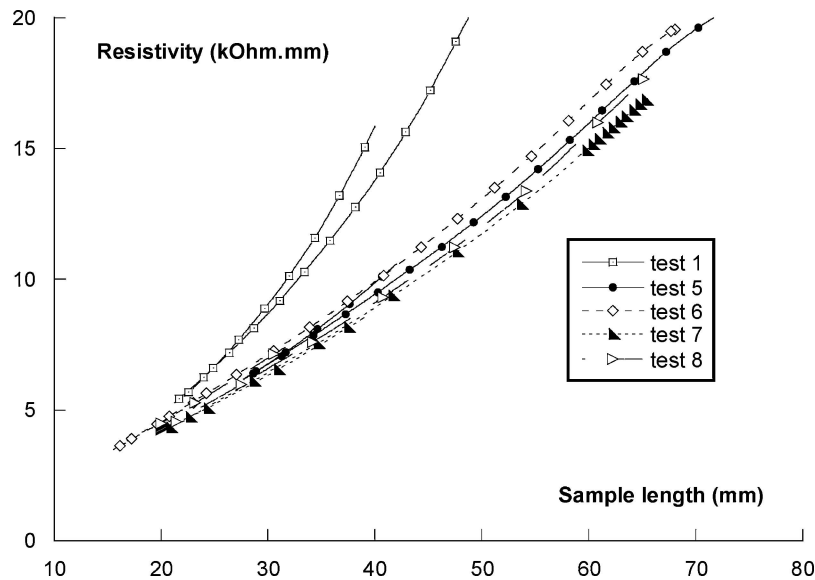


Figure 7 Mutton wool electrical resistivity as a function of sample length. Test 5–8 were carried out one day after test 1. Compression until 100 N at 6 mm/min.

wool, humid raw cotton and steel wool n°00000 in order to analyse the repeatability of the data collected (stress and electrical resistance). The first point to notice is that, except minor variation within the first quarter of the compression curve due to the arrangement of the carded fibres in the device, results show a good repeatability for the mechanical behaviour. Concerning electrical measurements, the results from steel wool are remarkably as stable as the mechanical response, while humidity of the laboratory air strongly influences the electrical conductivity of the organic materials and the results may vary from one day to the other. When performed during stable humidity atmospheric conditions, tests show a good repeatability (Fig. 7). It is worth noticing that the sample electrical resistivity is a reversible function of the sample length. The same curves are obtained with humid raw cotton. In the case of steel wool, the shape of the curves obtained

is different and some irreversibility appears (Fig. 8). This particular behaviour may be due to the local pliability of these fibres and to the irreversibility of such plastic deformation. However, the results obtained for the carbon nano tubes are similar to those of steel wool and more difficult to explain.

3.3. Cyclic tests

During cyclic deformation, the curves shifts with each successive cycle of load and unload but finally all the materials tested reaches a stable cycle shape after 2 or 3 cycles as illustrated on Fig. 9. After the first compression the morphology of the assembly and the motion at the contact/friction points have lead to a particular geometry. To explain this “ratcheting” effect, one can suppose that unloading and reloading would then just force fibres to bend but few motion of fibres would

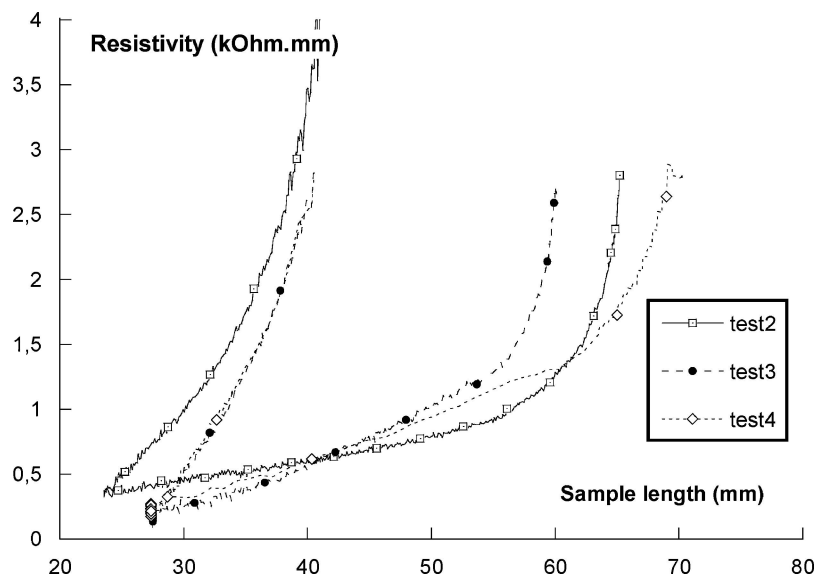


Figure 8 Steel wool n°00000 electrical resistivity as a function of sample length. Compression tests until 100 N at 6 mm/min.

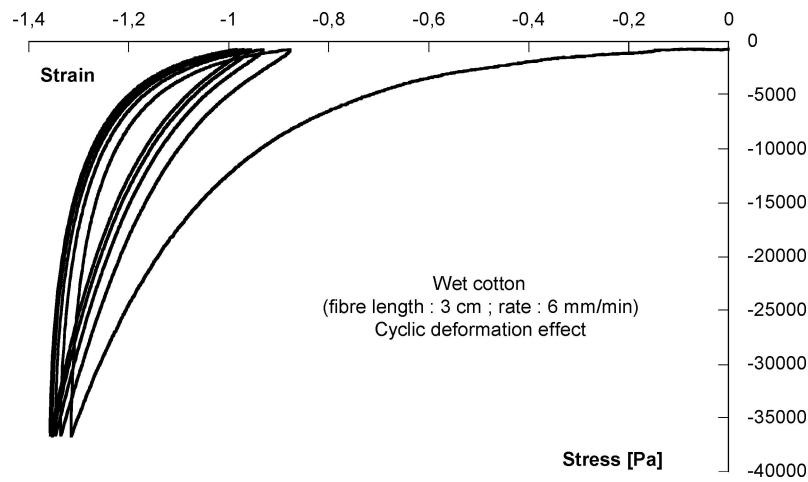


Figure 9 Humid raw cotton fibres of 3 cm. Cyclic compression tests until 100 N at 6 mm/min.

occur and the assembly would keep its microstructure. As the matted fibres have taken a certain shape after the first compression their ability to be compressed is largely reduced for the next cycle. This stabilisation of contact between fibres is confirmed by the electric measurement.

3.4. Strain rate effect

Three decades of strain rates (10^{-4} , 10^{-3} and 10^{-2} s $^{-1}$) have been explored for sheep wool, wick of cotton and steel wool. Time dependence of the mechanical behaviour is always evidenced (see Fig. 10a and b). The more slowly the test is performed, the more the set of fibres is compacted for the same load. This result is obtained for elastic wool (mutton wool and wick of cotton) but also for both steel wools. The effect of strain rate on the stress was also investigated during stress relaxation tests, the matt relaxes stress according to a logarithmic function of the time. Moreover, the amount of stress relaxed and the relaxation rate increase when the initial strain rate – before relaxation – is higher (Fig. 10b). The influence of strain rate on the motion of dislocation and the macroscopic plasticity is well

known [10, 11]. The influence of strain rate during the first compression stage of powder (when compaction is more due to the rearrangement of particles than to plastic deformation of particle) has also been studied [12]. Compaction induces very complex states of stress in the powder. Friction onto the device sample height, compaction rate and stress triaxiality strongly influence the compaction process. In the cases of entangled materials, the same tendency is evidenced in this study: time can help fibres motion and rearrangement, fibres with longer length induce more friction and are less compressed at the same load level. One of the key points is the number of contact between fibres and friction properties. This point is detailed in the next paragraph.

4. Discussion

The experimental set up allows to record the evolution of the mat fibre electrical resistance during the compression test. The purpose was to evaluate the number of contacts between entangled fibres. In fact, we get qualitative information but the electrical data collected do not allow us to quantify the number of fibre contacts: the electrical resistance of the assembly depends

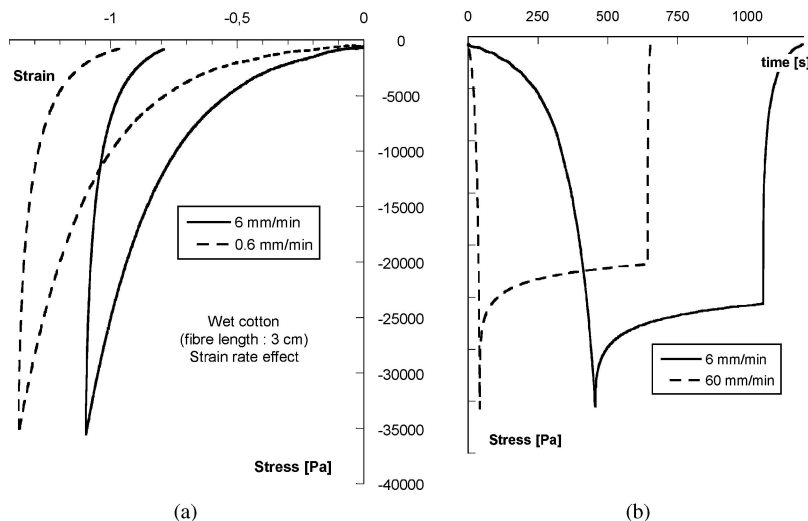


Figure 10 Strain rate effect on the mechanical behaviour (Maximum load 100 N): (a) humid cotton in simple compression test at two strain rate, (b) mutton wool during relaxation tests at two strain rate.

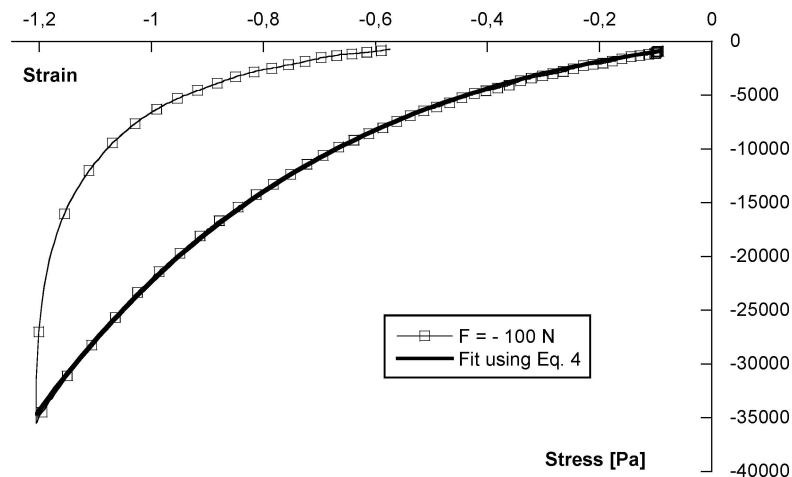


Figure 11 Compression test on mutton wool (6 mm/min until 100 N). Comparison of experimental data and modelling.

both on the number of contact and of the length of fibres. Electric conduction differs between the materials tested. For the steel wool, conduction occurs in the volume of the fibre, for mutton wool, electron transfer is due to mutton suet at the surface of the fibre as washed fibres is an insulator (in the range of electrical resistance tested). In test carried out with humid cotton fibres, conductivity is due to ionic conduction in the water. When spraying is performed with pure water, no electrical measurement can be achieved. Whatever the electrical conduction mode, the electrical resistance of the sample appears to depend mostly on the length of the specimen; short circuit from the top to the bottom of the sample appears to be the explanation of this behaviour. So the electrical measurements performed in this study give indication on the morphology of the assembly but cannot be linked to a number of contacts per volume unit.

Quantification of the number of contacts in such materials is a key point to perform modelling of the mechanical behaviour of entangled materials [6–9]. Micro-tomography of X-ray — has been used [13, 14] in order to get information on the morphology of such mattress of fibres but the method does not permit to get the number of contact or the distribution of distance between two contacts. From a macroscopic point of view, displacement field of a mattress of mineral fibres can be analysed and help to measure local strain field, to analyse crimp [15, 16]. The main difficulty is to get data at the microscopic scale: fibres diameter, distance between contacts . . . as they are necessary for modelling. On the other hand, macroscopic behaviour law [4] can be identified but they are not linked to physical parameters. It is claimed that loading and unloading curves can be fitted according to equation 4 but few studies are devoted to the understanding of such macroscopic law.

$$\sigma = a \varepsilon \cdot \exp(b \cdot \varepsilon) \quad (4)$$

The loading part of the compression curve of the mutton wool is nicely fitted using equation 4 as can be seen in Fig. 11. For this fit, the origin was set to the first point of the loading curve and we obtained the

parameters $a = 7786 \text{ Pa}$ and $b = -1.22$. The unloading part of the curve could not be fitted satisfactorily. In 1946, Van Wyk proved that the compression of a mass of wool fibres consists solely of the bending of the fibres [17]. But this analysis cannot explain the hysteresis loop between loading and unloading and friction at the contact point must be taken into account.

5. Conclusion

Experiments on various set of fibres in compression have been carried out and a master curve is evidenced. Electric resistance gives indication about the arrangement of fibres but the number of contacts and the distance between contact cannot be deduced from these measurements whereas it is a key point to improve modelling of the behaviour of these materials. Mechanical behaviour of such materials is due to the morphology of the assembly and to motion, friction and rearrangement of the fibres during the compaction. The strong hysteresis in the macroscopic behaviour has to be linked with the friction law at the contact point more than to inelastic behaviour of the fibres. More work has to be done to increase the experimental set of data in order to model the mechanical behaviour of these complex materials with acceptable physical basis.

Acknowledgements

The authors would like to thank Philippe SERP and Marius VIGUIER for providing respectively carbon nano tubes and raw mutton fibres.

References

1. L. J. GIBSON and M. F. ASHBY, in "Cellular Solids: Structure and Properties" (Cambridge University Press, Cambridge, 1997).
2. M. F. ASHBY, A. G. EVANS, N. A. FLECK, L. J. GIBSON, J. W. HUTCHINSON and H. N. G. WADLEY, 1, in "Metal foams: A Design Guide" (Butterworth Heinemann, Boston, 2000).
3. P. CASTERA, "Comportement physico-mécanique des matériaux fibreux celluloseux considéré comme des milieux aléatoires", in Proceeding of Matériaux 2002, 21–25 Oct, 2002 (Tours, France, CM02077).
4. J.-M. HAEFFELIN, F. BOS AND P. CASTERA "Modélisation du comportement d'un matelas de fibres celluloseux au cours de sa consolidation," in Proceeding of Matériaux 2002, 21–25 Oct 2002 (Tours, France, CM02022).

MECHANICAL BEHAVIOR OF CELLULAR SOLIDS

5. M. BAUDEQUIN, 'Identification des mécanismes physiques mis en jeu lors de la reprise d'épaisseur de la laine de verre,' (Thèse, Université Pierre et Marie Curie Paris VI, 2002).
6. D. RODNEY, M. FIVEL and R. DENDIEVEL, "Discrete Modelling of the Mechanical Behaviour of Entangled Fibrous Materials", Poster EUROMECH Colloquium 459 Mechanical behaviour of cellular solids. 7–10 June 2004, Nancy, France.
7. D. DURVILLE, "Modelling of Contact-Friction in Entangled Fibrous Materials," in Proceeding of Computational Mechanics WCCM VI, Sept. 5–10, Beijing, China (2004).
8. D. DURVILLE, "Finite Element Modelling of the Nonlinear Behaviour of Fibrous Materials Considering Internal Contact-Friction Interactions," in Proceeding of the European Congress on Computational Method in Applied Sciences and Engineering (ECCOMAS 2004), 24–28 July 2004, Jyväskylä.
9. C. R. HASELEIN, Numerical Simulation of Pressing Wood-Fiber Composites,' Ph. D. Thesis, Oregon State University, USA, 1998.
10. 'Dislocations et Déformation Plastique', In Proceedings of Summer School, Yrvals, 3–14 Sept. 1979, Edited by P. Grok, L. P. Kubin and J.-L. Martin (Les éditions de Physique, Les Ulis, France, 1980).
11. F. R. N. NABARRO, *Phil. Mag.* **83** (23) (2003) 3047.
12. J. A. LUND, *Int. J. Powder Metallurgy* **18** (2) (1982) 117.
13. M. FAESSELL, C. DELISSÉE, P. CASTÉRA and J. LUX, "Caractérisation et modélisation 3D de matériaux fibreux cellulosiques à partir d'imagerie par micro-tomographie X" in Proceeding of Matériaux 2002, 21–25 Oct 2002, (Tours, France, CM02024).
14. C. DELISÉE, D. JEULIN and F. MICHAUD, *C.R. Académie Sciences* **329**, Série IIB (2001), 179.
15. F. HILD, B. RAKA, M. BAUDEQUIN, S. ROUX and F. CANTELAUBE *Applied Optics*, **41** (31) (2002) 6815.
16. S. BERGONNIER, F. HILD and S. ROUX, "Mechanical Behaviour of Crimped Glass Wool," EUROMECH Colloquium 459 Mechanical behaviour of cellular solids. (7–10 June 2004), Nancy, France.
17. C. M. VAN WYK, *J. Textile Institute* **37** (1946) 285.

*Received December 2004
and accepted April 2005*